JOURNAL OF CATALYSIS 22, 226–236 (1971)

Hydrogenolysis and Isomerization of *n*-Pentane on Group VIII Transition Metals

EIICHI KIKUCHI, MICHIO TSURUMI, AND YOSHIRO MORITA

Department of Applied Chemistry, School of Science and Engineering, Waseda University, Tokyo, Japan

Received October 6, 1970

The reaction of *n*-pentane in the presence of hydrogen was studied using supported Group VIII transition metals as catalyst. The specific activity for hydrogenolysis referred to unit surface area of the metal was examined and the following sequence was obtained: Ru > Rh > Pt > Ni > Co > Ir > Pd ~ Fe.

Hydrogenolysis on nickel proceeded via successive demethylation at the terminal carbon–carbon bond of adsorbed hydrocarbon, whereas on cobalt and iron, the desorption step of surface residues was so slow that the exact mode of hydrogenolysis could not be determined. On Group VIII noble metals, all the carbon–carbon bonds of *n*-pentane cracked almost statistically. On ruthenium, rhodium, and iridium, multiple bond breaking (extensive degradation) occurred at low partial pressure of hydrogen, although at high partial pressure of hydrogen, the amounts of methane and ethane were equal, respectively, to those of butane and propane. The main features of the product distributions of hydrogenolysis on palladium and on platinum catalysts could be accounted for by assuming that only one carbon–carbon bond was ruptured at the residence of a molecule on the surface. Carbon-supported catalysts produced methane and butane in higher proportion than silica gel supported catalysts.

Among all the Group VIII transition metals with the exception of osmium, only palladium and platinum were found to be active for isomerization of *n*-pentane to isopentane. The selectivity of platinum for isomerization was found to decrease with increasing partial pressure of hydrogen.

INTRODUCTION

Studies on the catalytic hydrogenolysis of small paraffinic hydrocarbons over supported metal catalysts have been summarized in a recent review (*1*). Ethane hydrogenolysis over a series of Group VIII transition metals was investigated in detail by Sinfelt and Yates (*2*, *3*), and the activity sequence was found to be related to electronic and geometric factors. These kinetic studies were interpreted in terms of a reaction scheme originally proposed by Cimino, Boudart, and Taylor (*4*).

Investigations relating to the product distributions from the hydrogenolysis of larger hydrocarbons have been reported by Anderson and Baker (Ni, Rh, W, Pt) (*5*, *6*), Anderson and Avery (Pt and Pd) (*7*–*9*), Kochloefl and Bazant (Ni) (*10*), Kempling and Anderson (Ru) (*11*) and Kikuchi and Morita (*12*). There exists, however, no detailed information concerning the selectivities of individual Group VIII metals in the carbon–carbon bond splitting of larger paraffins. The hydrogenolysis of *n*-pentane on supported nickel catalyst has been previously reported (*12*). The authors have now extended their studies to the reaction of *n*-pentane in the presence of hydrogen using supported-Group VIII metal catalysts. The main purpose of the present work was to determine the selectivities of all the Group VIII metals except osmium in hydrogenolysis of

n-pentane, and to clarify the effects of hydrogen pressure and temperature on the product distribution. Osmium was excluded because of its tendency to form the volatile, toxic oxide OsO_4.

It has been also found that some of these metals are active for skeletal isomerization of paraffins. Anderson and Avery (*7*) found that isomerization of isopentane and neopentane took place on platinum and palladium films (palladium was less active than platinum) in which the metal was the sole seat of catalytic activity. Later Maire, Gault *et al.* (*13–15*) showed that hydrocarbon could be isomerized on platinum via a cyclic intermediate, a cyclopentane, or a cyclopropane intermediate. More recently Boudart and Ptak (*16*) found that, as well as on platinum and gold, skeletal isomerization took place on iridium which Anderson and Avery believed to be inactive. Thus it was also the intention of this work to determine on what metals, straight chain pentane (*n*-pentane) would be isomerized. The gross kinetics of both reactions, hydrogenolysis and isomerization were determined.

Experimental

Apparatus and Procedure

The kinetic studies were made in a flow reactor system whose details were described in our previous paper (*12*). All the reaction products were paraffins containing one to five carbon atoms in the molecule, and were analyzed by gas chromatography using a 6-m column of tetraisobutylene (at room temperature).

The catalyst (30–400 mg) was packed at the central position of the reactor and was reduced at 450°C for 2 hr in a stream of hydrogen prior to reaction.

Reaction was carried out in the temperature range of 260–400°C, and at total pressure of 2.5–70 atm. Feed rate of *n*-pentane was in the range of 1.74×10^{-4}–6.96×10^{-3} moles/min, and molar ratio of flows of hydrogen to *n*-pentane was changed over the range 5–140. About 5 min were required to reach steady state of the reactor system, and the effluent gas in the following 10 min was analyzed.

The surface areas of metals were determined by chemisorption of hydrogen at 20°C, except for palladium; here surface area was determined by chemisorption of carbon monoxide at 20°C. A conventional glass vacuum system was used for isotherm measurements. The weight of the sample used for chemisorption measurement was approximately 3 g. Prior to the measurement of an isotherm, the catalyst sample was reduced *in situ* in the flowing hydrogen for 2 hr at 450°C. After evacuation at the same temperature for 2 hr, the sample was cooled to room temperature for the measurement. A period of 60 min was found to be sufficient to attain equilibrium in the determination of a point of an isotherm, and the amount of gas adsorbed at 10 cm Hg pressure was taken as the monolayer point.

Materials

The supported catalysts used in the present work contained 5 wt % of metal. Fe/SiO_2, $Co–SiO_2$, $Ni–SiO_2$, $Ru–SiO_2$, $Rh–SiO_2$, $Pd–SiO_2$, $Ir–SiO_2$, and $Pt–SiO_2$ catalysts were prepared by individually impregnating silica gel with solution of $Fe(NO_3)_3 \cdot 9H_2O$, $Co(NO_3)_2 \cdot 6H_2O$, $Ni(NO_3)_2 \cdot 6H_2O$, $RuCl_3$, $RhCl_3$, $PdCl_2$, $IrCl_4$, and $H_2PtCl_6 \cdot 6H_2O$. Silica gel used as support was the same as that described previously (*12*), being catalytically neutral. Pt–C catalyst was prepared in the same method using activated carbon powder as support instead of silica gel. These catalysts were dried and calcined at 500°C for 2 hr, with the exception of $Ru–SiO_2$. The ruthenium catalyst was dried in a dessicator prior to weighing because of the possibility of forming volatile oxide at higher temperatures. The carbon powder used as support, as well as Ru–C and Rh–C catalysts were obtained from Nippon Engelhard Ltd. The ruthenium trichloride, rhodium trichloride, palladium dichloride, and chloroplatinic acid were also obtained from Nippon Engelhard

Ltd. Other metal salts were obtained from Japan Pure Chemicals, Inc.

The pentane used in this work was a commercial reagent designated as GR Grade (Japan Pure Chemicals, Inc.), and no detectable amount of impurities was included in it. Cylindrical hydrogen was used after purification through Deoxo unit to remove oxygen impurity. The water formed was then removed by a molecular sieve drier.

Results and Discussion

The Activity of Group VIII Transition Metals

Hydrogenolysis of *n*-pentane over a series of Group VIII metals was studied in the partial pressure range of 0.5–2.0 atm for *n*-pentane, and of 2.5–70 atm for hydrogen. A typical relation between conversion of *n*-pentane (X) and the time factor (W/F) is shown in Fig. 1. The conversion of *n*-pentane was defined as in the previous paper (*12*);

$$X = \frac{(-\Delta P_{C_5})}{P_{C_5}^0}, \qquad (1)$$

where $(-\Delta P_{C_5})$ and $P_{C_5}^0$ are the decrease of *n*-pentane partial pressure and initial pressure of *n*-pentane, respectively. The usual reciprocal space velocity was used as the time factor, W/F, where W and F were catalyst weight (g) and feed rate of *n*-pentane (mole/min), respectively. As shown in this figure, reaction was suppressed by hydrogen. This trend was common for all the other catalysts.

The initial rate of *n*-pentane disappearance (V) defined as in Eq. (2) was obtained from the initial gradient of conversion vs. the time factor, and was fitted to a simple power expression (3).

$$V = \frac{dX}{d(W/F)}, \text{ and} \qquad (2)$$

$$V = k(P_{C_5}^0)^m(P_{H_2}^0)^n. \qquad (3)$$

A typical relation between rate of *n*-pentane disappearance and partial pressure of *n*-pentane and hydrogen is shown in Fig. 2. The inclusion of terms for the partial

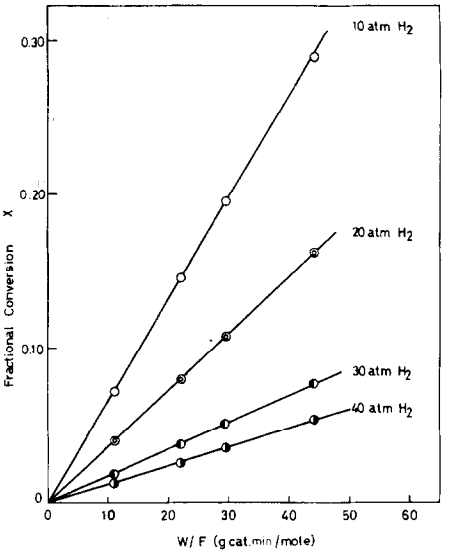

FIG. 1. A typical relation between fractional conversion and reciprocal space velocity (W/F) on a Pt–SiO_2 catalyst at 430°C, partial pressure of *n*-pentane 0.5 atm, and various partial pressures of hydrogen: ○, 10 atm; ◎, 20 atm; ◐, 30 atm; ◑, 40 atm.

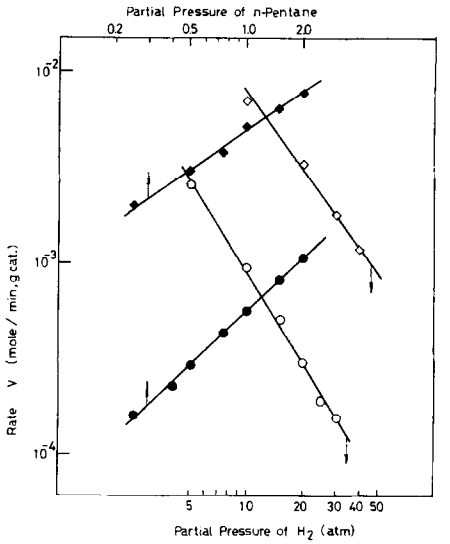

FIG. 2. Effect of the partial pressure of hydrogen and *n*-pentane on the rate of *n*-pentane hydrogenolysis: at 430°C, partial pressure of *n*-pentane 0.5 (◇), and partial pressure of hydrogen 20 atm (◆) on a Pt–SiO_2 catalyst; at 350°C, partial pressure of *n*-pentane 0.5 atm (○), and partial pressure of hydrogen 20 atm (●) on a Ni–SiO_2 catalyst.

pressure of the products did not significantly improve the correlation, so they were deleted. Table 1 summarizes the kinetic parameters, where the rate is expressed in moles of *n*-pentane reacted/m^2 of metal min^{-1} and pressure in atm.

The experimentally determined surface areas of the metals are also given in Table 1. In spite of similar method of preparation of catalysts, there was almost an order of magnitude difference between the most dispersed metal (10.1 m^2/g-cat.) and the least dispersed (0.5 m^2/g-cat.). The relative areas of the metals in the silica-supported catalysts of Sinfelt and Yates (*1*) showed a similar trend, and the metal surface areas of our catalysts were not greatly different from theirs.

Arrhenius plots for specific rate constant, k_s, which is obtained by dividing k by metal surface area are given in Fig. 3. Activation energies and pre-exponential factors in the equation $k_s = A \exp(-E/RT)$ are also shown in Table 1.

From the results shown in Fig. 3, the approximate order of catalytic activity is determined as follows: Ru > Rh > Pt > Ni > Co > Ir > Pd ~ Fe. This activity sequence is almost the same as that for ethane hydrogenolysis observed by Sinfelt *et al.* (*1*), except for platinum of which the activity sequence in *n*-pentane hydrogenolysis is somewhat higher than that in ethane hydrogenolysis. The observed activation energies were compared with those for ethane hydrogenolysis, as in Fig. 4. A satisfactory linear relation is observed between them except for platinum catalyst. For the hydrogenolysis on nickel, iron, ruthenium, or rhodium (*4*, *6*, *11*), 1,2-diadsorbed species have been proposed. For platinum, however, strong evidence for 1,3-diadsorbed intermediates has been presented by Anderson and Avery (*8*) and Boudart *et al.* (*17*). The difference in the adsorbed state would be one of the possible interpretations for low activation energy experimentally observed for platinum catalyst.

The Selectivity in Hydrogenolysis

In the previous paper (*12*), we reported that the product distributions of *n*-pentane hydrogenolysis on nickel catalyst could be explained in terms of a mechanism including successive demethylation on the nickel surface. According to this scheme, only methane and *n*-butane are the initial products from *n*-pentane hydrogenolysis at low temperature and/or at high partial

TABLE 1

KINETIC PARAMETER FOR *N*-PENTANE HYDROGENOLYSIS

$V_s = k_s$ (pentane pressure)^m (hydrogen pressure)^n

Catalyst	Metal surface area (m^2/g-cat.)	m[a]	n[b]	Apparent activation energy (kcal/mole)	A[c]
$Fe-SiO_2$	0.5	0.5	−0.6	23.4	4.79×10^4
$Co-SiO_2$	1.3	0.9	−1.5	30.9	1.35×10^9
$Ni-SiO_2$	2.8	0.9	−1.6	31.2	1.95×10^9
$Ru-SiO_2$	4.3	0.9	−1.6	29.1	2.09×10^{11}
Ru–C	5.6	1.0	−1.5	37.2	1.02×10^{14}
$Rh-SiO_2$	8.9	1.0	−1.3	30.4	7.76×10^9
Rh–C	10.1	1.0	−1.3	31.1	5.37×10^9
$Pd-SiO_2$	1.1	0.9	−1.4	49.2	2.29×10^{13}
$Ir-SiO_2$	7.3	1.0	−1.5	32.0	1.55×10^9
$Pt-SiO_2$	0.8	0.7	−1.4	27.6	8.14×10^8
Pt–C	0.9	0.8	−1.4	33.6	2.95×10^9

[a] Obtained in the range of 0.25–2.0 atm.

[b] Obtained in the range of 5–40 atm.

[c] Rate was expressed in mole/min, m^2 of metal.

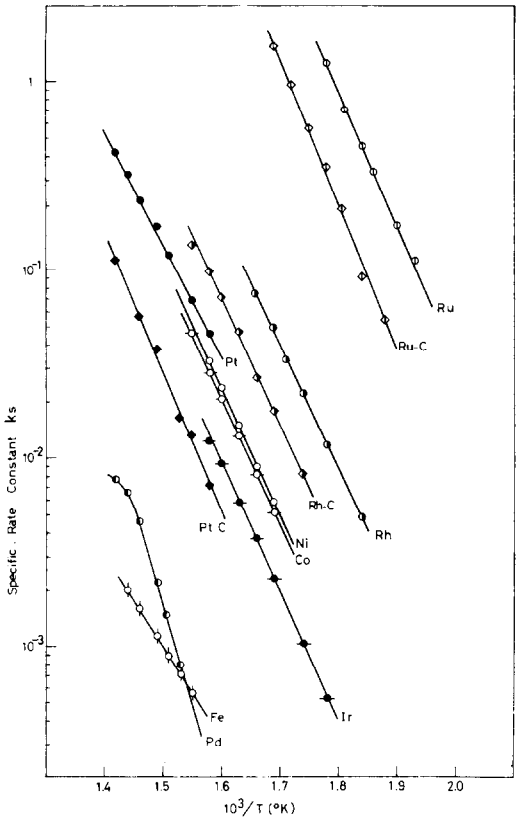

FIG. 3. Arrhenius plots for the specific rate constant of *n*-pentane hydrogenolysis on supported Group VIII metals: ○, Fe-SiO_2; -○-, Co-SiO_2; ○, Ni-SiO_2; ◫ (◈), Ru-SiO_2 (Ru-C); ◑, (◆), Rh-SiO_2 (Rh-C); ◐, Pd-SiO_2; -●-, Ir-SiO_2; ● (◆), Pt-SiO_2 (Pt-C).

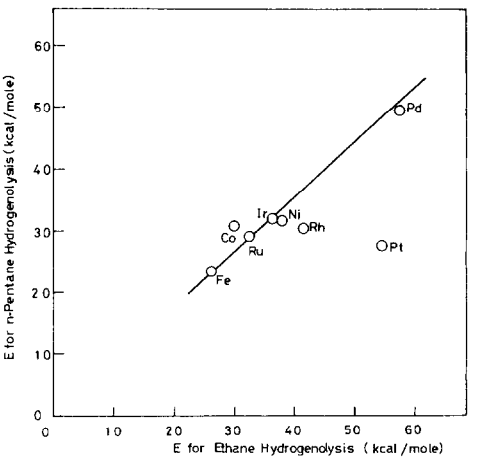

FIG. 4. Correlation of the apparent activation energy for *n*-pentane hydrogenolysis with that for ethane hydrogenolysis (adopted from Ref. *1*) on silica-supported Group VIII metals.

pressure of hydrogen. At low partial pressure of hydrogen, however, multiple bond breaking (extensive degradation) occurs before desorption of adsorbed species, for example one propane and two methane from one pentane.

The product distributions of *n*-pentane hydrogenolysis were determined at various conditions of reaction temperature and partial pressure of hydrogen. The selectivity of each product was defined as the moles of that product produced divided by the moles of *n*-pentane reacted.

$$\text{Selectivity of } C_nH_{2n+2},\ S_{C_n} = \frac{5C_n}{C_1 + 2C_2 + 3C_3 + 4(\text{iso-}C_4 + n\text{-}C_4) + 5\ \text{iso-}C_5} \quad (4)$$

Extrapolation of these values to zero conversion gave the initial product distribution without subsequent cracking of products. Typical results are summarized in Table 2.

The product distributions for cobalt and iron catalysts at these conditions were very similar to those for nickel catalyst at low partial pressure of hydrogen. Particularly with iron catalyst, very few hydrogenolysis products other than methane are formed under these conditions. Larger hydrocarbon species undergo hydrogenolysis appreciably faster than they desorb. This reconciled with low activation energy and small values of reaction order with respect to *n*-pentane (m), since these values suggested strongly adsorbed hydrocarbon on this catalyst.

In hydrogenolysis on ruthenium catalysts, splitting of central carbon–carbon bonds (bisecondary CH_2—CH_2) of *n*-pentane was observed in addition to terminal bond rupture. A typical relation between initial product distributions and partial pressure of hydrogen is illustrated in Fig. 5. Selectivities for all the products converged on 0.5 by increasing partial pressure of hydrogen. Thus each carbon–carbon bond has about the same prob-

TABLE 2
TYPICAL DATA FOR THE INITIAL PRODUCT DISTRIBUTION

Catalyst	Temperature (°C)	Partial pressure of *n*-pentane (atm)	Partial pressure of hydrogen (atm)	Initial selectivity for				
				CH_4	C_2H_6	C_3H_8	n-C_4H_{10}	iso-C_5H_{12}
Fe–SiO_2	370	0.5	20	4.3	0.09	0.18	—	—
	390	0.5	20	4.5	0.06	0.12	—	—
	400	0.5	20	5.0	—	—	—	—
	400	0.5	40	5.0	—	—	—	—
Co–SiO_2	330	1.0	30	3.2	0.21	0.18	0.22	—
	350	0.5	5	3.9	0.18	0.12	0.09	—
	350	0.5	30	2.9	0.32	0.13	0.46	—
	360	1.0	30	3.6	0.25	0.15	0.13	—
Ni–SiO_2	330	0.5	15	1.3	0.03	0.18	0.77	—
	350	0.5	5	3.4	0.19	0.19	0.14	—
	350	0.5	15	1.6	0.10	0.30	0.56	—
	350	0.5	30	1.0	—	—	1.0	—
	370	0.5	15	2.3	0.18	0.33	0.35	—
Pd–SiO_2	400	1.0	20	0.40	0.41	0.40	0.40	0.19
	430	0.5	10	0.51	0.22	0.21	0.49	0.26
	430	0.5	20	0.45	0.28	0.28	0.45	0.26
	430	0.5	30	0.43	0.33	0.33	0.43	0.26
Pt–SiO_2	390	0.5	20	0.48	0.55	0.56	0.43	—
	430	0.5	5	0.25	0.43	0.40	0.25	0.33
	430	0.5	10	0.35	0.54	0.50	0.33	0.15
	430	0.5	20	0.39	0.61	0.61	0.39	0.08
Pt–C	360	1.0	20	0.67	0.35	0.33	0.64	0.01
	380	1.0	20	0.62	0.36	0.34	0.61	0.04
	430	0.5	5	0.42	0.33	0.33	0.42	0.25
	430	0.5	10	0.51	0.33	0.33	0.51	0.15
	430	0.5	20	0.59	0.33	0.33	0.59	0.08

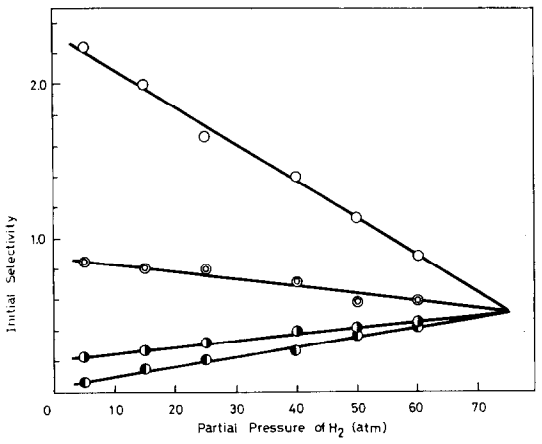

FIG. 5. Dependence of the initial selectivity for each product of *n*-pentane hydrogenolysis over a Ru–C catalyst on the partial pressure of hydrogen at 300°C, partial pressure of *n*-pentane 0.5 atm: ○, methane; ◎, ethane; ◑, propane; ◐, *n*-butane.

ability of being cracked, i.e., the hydrogenolysis is unselective with respect to bond type at high partial pressure of hydrogen. The selectivity data were plotted against the difference between selectivity for methane and that for *n*-butane, $S_{C1} - S_{C4}$ (see Fig. 6). The overlap of data taken with Ru–C and Ru–SiO_2 catalysts and at different temperatures near 300°C or partial pressure of hydrogen suggested that the unselective rupture of carbon–carbon bonds is characteristic of ruthenium metal. This agrees with the observation by Kempling and Anderson (*11*) for hydrogenolysis of *n*-butane on ruthenium-alumina catalyst.

A typical result of *n*-pentane hydrogenolysis on Rh–C catalyst is shown in Fig. 7, in which the selectivities for each product are plotted against conversion of

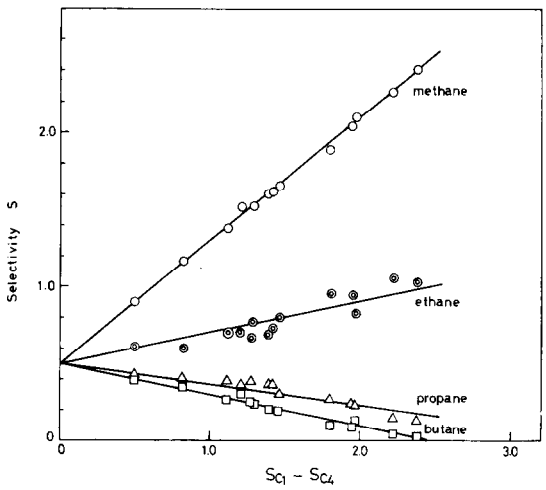

FIG. 6. Product distribution of *n*-pentane hydrogenolysis on ruthenium catalysts vs. S_{c_1}—S_{c_4}.

n-pentane. The selectivities of *n*-butane and propane decreased with increasing conversion, while those of methane and ethane increased. Thus at higher conversions some of the initial products returned to the catalyst for further reaction. Extrapolation of the selectivity data at this condition to zero conversion gave the relation: $C_1 = C_4$, $C_2 = C_3$.

The rupture of carbon–carbon bonds on rhodium catalyst, however, was found to be selective with respect to bond type. The relations between the initial selectivities for each product and partial pressure of hydrogen are given in Fig. 8 for Rh–C and Rh–SiO_2 catalysts. The splitting of inner carbon–carbon bonds of *n*-pentane occurred in larger proportion than that of outer ones. Data shown in Fig. 8 suggested that the proportion depended on the nature of support used. The selectivity of the carbon–carbon bond breaking was little influenced by reaction temperature. With neohexane, it was found by Anderson and Baker (*5*, *6*) that carbon–carbon bond in ethyl group was selectively broken on rhodium catalyst. Thus, the carbon–carbon bond of quaternary carbon atom would have to be of little reactivity in hydrogenolysis on rhodium.

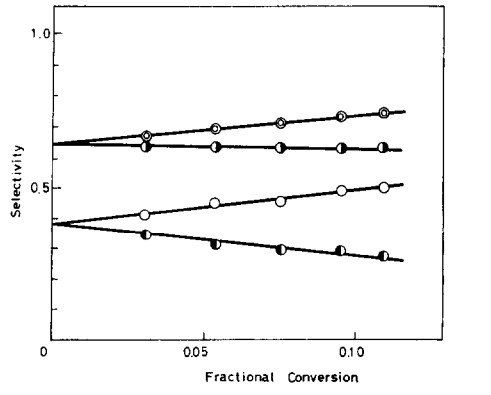

FIG. 7. Dependence of selectivity for *n*-pentane hydrogenolysis products on fractional conversion of *n*-pentane at 350°C, partial pressure of *n*-pentane 0.5 atm, partial pressure of hydrogen 50 atm on a Rh–C catalyst: ○, methane; ◎, ethane; ◑, propane; ◐, *n*-butane.

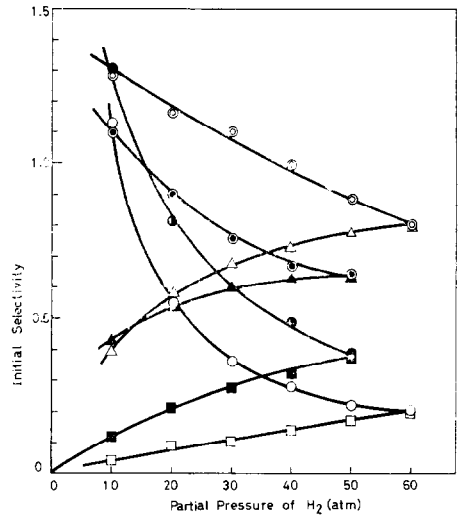

FIG. 8. Variation of the initial product distributions with the partial pressure of hydrogen at 350°C, partial pressure of *n*-pentane 0.5 atm on a Rh–SiO_2 (a Rh–C) catalyst: ○ (●), methane; ◎ (◉), ethane; △ (▲), propane; □ (■), *n*-butane.

The pattern of carbon–carbon bond rupture on iridium catalyst was found to be very similar to that for rhodium catalyst. A typical result for selectivity of iridium catalyst is shown in Fig. 9. Skeletal isomerization of *n*-pentane was not observed on this catalyst in the temperature range studied (300–400°C), although Boudart and Ptak (*16*) found it in the reaction of neopentane.

On ruthenium, rhodium, and iridium

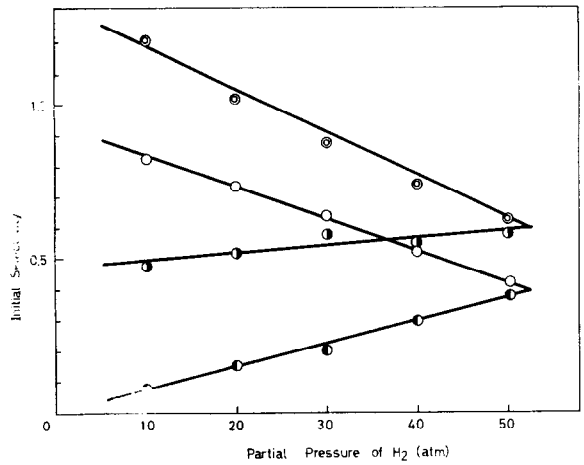

FIG. 9. Variation of the initial product distributions with the partial pressure of hydrogen at 350°C, partial pressure of *n*-pentane 0.5 atm on Ir-SiO_2 catalyst: ○, methane; ◎, ethane; ◑, propane; ◐, *n*-butane.

catalysts, multiple bond breaking was found to occur extensively at low partial pressure of hydrogen (see Figs. 5, 8, and 9).

On palladium and platinum, however, the smallest proportion of multiple bond breaking was observed, even at low-hydrogen partial pressure. Furthermore, the product distributions were almost constant in the fractional conversion range of 0–0.2 (see Fig. 10). The main features of the distributions of hydrogenolysis products given in Fig. 10 and Table 2 may be accounted for on the assumption that, in any particular molecule on the surface, only one carbon–carbon bond is broken on these catalysts. With these catalysts, skeletal isomerization to isopentane was found to proceed in parallel with hydrogenolysis.

With both rhodium and platinum catalysts, the proportion of rupture at inner carbon–carbon bond on a silica-supported catalyst was larger than that on carbon-supported ones.

Hydrogenolysis on nickel proceeds via successive demethylation from the terminal carbon–carbon bond of surface residues (*12*). On iron and cobalt, desorption of surface residues appears to be so slow that the exact mode of hydrogenolysis cannot be determined. The distributions of hydrogenolysis products on these catalysts were similar to those obtained with nickel catalyst at low partial pressure of hydrogen or at high temperature. Then from comparison with the features of the product distributions of hydrogenolysis on nickel catalyst, it may be deduced that the successive demethylation mechanism also operates in the case of iron and cobalt

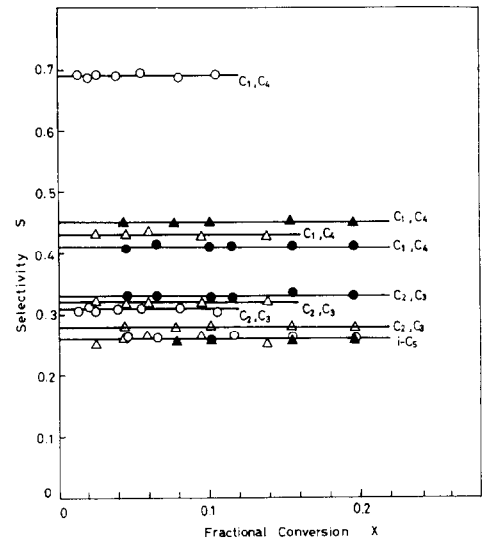

FIG. 10. Dependence of selectivities for *n*-pentane hydrogenolysis products on fractional conversion of pentane at 430°C, partial pressure of pentane 0.5 atm: partial pressure of hydrogen 5 atm (●) and 30 atm (○) on a Pt–C catalyst; partial pressure of hydrogen 20 atm (▲) and 30 atm (△) on a Pd-SiO_2 catalyst.

catalysts, desorption of surface residues being slow. On the other hand, rupture of bisecondary CH_2—CH_2 bond to produce equal amounts of ethane and propane apparently occurred on the noble metals of Group VIII. From the results of hydrogenolysis of ethane, Sinfelt and Yates (*1–3*) concluded that the noble and nonnoble metals showed different patterns of catalytic behavior. It was revealed that the hydrogenolysis activity increased with increasing percentage *d*-character of the metal bond (electronic factor), and that the metals of the second triad (Ru, Rh, Pd) and the third triad (Os, Ir, Pt) gave a satisfactory correlation line when the catalytic activity was related to the percentage of *d*-character. However, the data for the nonnoble metals, namely the metals of the first triad (Fe, Co, Ni) were found to deviate distinctly from the correlation line for the noble metal. The difference between the noble and nonnoble metals was interpreted by introducing one more factor (geometric factor). As mentioned above, the distinction between the noble and nonnoble metals is also evident in the rupture modes of carbon–carbon bond in *n*-pentane hydrogenolysis.

The Selectivity in Isomerization

The skeletal isomerization of paraffin on Group VIII transition metals has been observed with iridium and platinum for neopentane (*16*) and with palladium (its selectivity being very low) and platinum for isopentane (*7*). In the present work it was found that only palladium and platinum among the metals studied were active for isomerization of *n*-pentane to isopentane. It was also shown that selectivity of platinum for isomerization was considerably influenced by the reaction conditions such as temperature or partial pressure of hydrogen, whereas the selectivity of palladium catalyst was almost independent of them.

As isomerization proceeded in parallel with hydrogenolysis, conversion by isomerization X_I was expressed as

$$X_I = \frac{\Delta P_{\text{iso-C}_5}}{P_{C_5}^0}, \qquad (5)$$

where $P_{\text{iso-C5}}$ is partial pressure of isopentane. The rates of isomerization were obtained from Eq. (2) with X_I instead of X. The selectivity for isomerization was defined by the ratio of the initial rate of isomerization to that of *n*-pentane disappearance V_I/V.

Data for the dependence of selectivity for isopentane formation on partial pressure of hydrogen are summarized in Table 2. The selectivity of platinum for isomerization decreased with increasing partial pressure of hydrogen. This showed that isomerization was more strongly suppressed by hydrogen on this catalyst than was hydrogenolysis. The selectivity of palladium catalyst was found to be almost independent of hydrogen pressure. The reaction orders for isomerization are given in Table 3.

Arrhenius plots for the specific rate constants of isomerization ($k_{I,s}$) are shown in Fig. 11. Activation energies and preexponential factors derived therefrom are listed in Table 3.

For the metals, especially in the case of iridium where no isopentane formation was observed, we can not say without further work that these catalysts are inactive for isomerization of *n*-pentane. As mentioned above, isomerization proceeded

TABLE 3

KINETIC PARAMETERS FOR *n*-PENTANE ISOMERIZATION

$V_{I,s} = k_{I,s}$ (pentane pressure)$^{m'}$ (hydrogen pressure)$^{n'}$

Catalyst	m'[a]	n'[b]	Apparent activation energy (kcal/mole)	A_I[c]
Pd–SiO_2	0.9	−1.4	49.2	4.88×10^{12}
Pt–SiO_2	1.0	−2.7	53.2	1.12×10^{16}
Pt–C	1.0	−2.2	56.6	5.37×10^{16}

[a] Obtained in the range of 0.25–2.0 atm.

[b] Obtained in the range of 5–20 atm.

[c] Rate was expressed in mole/min, m^2 of metal.

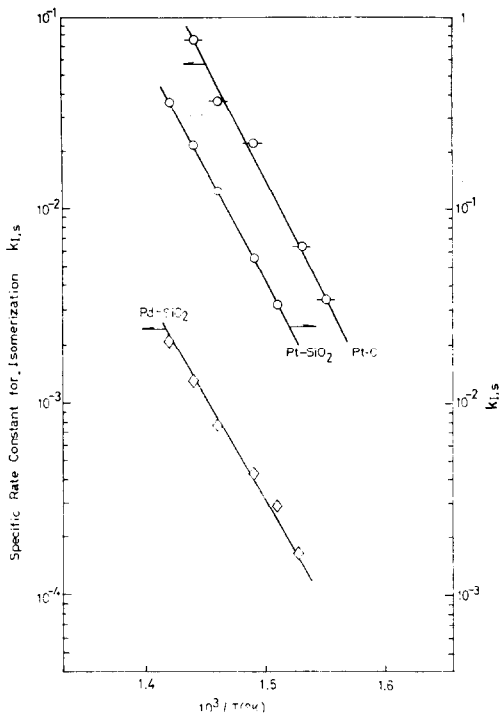

FIG. 11. Arrhenius plots for the specific rate constant of *n*-pentane isomerization on palladium and platinum catalysts: ◇, Pd–SiO_2; ○, Pt–SiO_2; –○–, Pt–C.

in parallel with hydrogenolysis. Anderson and Avery (*8*) showed that the products of both isomerization and hydrogenolysis were formed concurrently from a common surface intermediate. For neopentane the activation energies of isomerization are, as observed by Boudart and Ptak (*16*), almost comparable with those for hydrogenolysis. For *n*-pentane isomerization, however, the activation energies were higher than those for its hydrogenolysis. These results suggested that *n*-pentane was more readily destroyed by hydrogenolysis than neopentane. It is interesting that on platinum and palladium (active for isomerization of *n*-pentane) the residence of a molecule on the surface resulted in the rupture of not more than one carbon–carbon bond, whereas on other catalysts, multiple bond breaking was observed to an appreciable extent. Thus it would be that the isopentane formed was destroyed by hydrogenolysis very rapidly on the metals which appeared to be inactive for the isomerization of *n*-pentane.

Anderson and Avery (*8*) have proposed that in isomerization of aliphatic hydrocarbons on platinum, the hydrocarbon must be 1,3-diadsorbed with one sp^2 carbon forming a double bond with a surface atom. And it was also suggested from Hückel MO calculations that there is partial electron transfer from the adsorbed hydrocarbon to the surface metal atom (*8*). Boudart and Ptak (*16*) found that only iridium, platinum, and gold isomerized neopentane to isopentane, and they speculated that the exceptional ability of these three metals to isomerize neopentane is related to their high electronegativity and to a readily-shifted surface valency. These considerations indicated that electronic properties of metal atom have strong effects on the selectivity to isomerization. Therefore, we attempted to examine the ability of finely dispersed transition metals for isomerization of *n*-pentane. One of the results showed that *n*-pentane was isomerized with highly enhanced selectivity on sodium Y-zeolite exchanged by palladium and platinum, where the finely dispersed metals surrounded by framework oxygen of high electronegativity would be cationic (electron deficient). These results will be published separately.

ACKNOWLEDGMENT

This work was sponsored by Nippon Engelhard Ltd. It is a pleasure to thank Nippon Engelhard Ltd. for their generous gift of catalysts and the characterization of several of them.

REFERENCES

1. SINFELT, J. H., *Catal. Rev.* **3**, 175 (1970).
2. SINFELT, J. H., AND YATES, D. J. C., *J. Catal.* **8**, 82 (1967).
3. SINFELT, J. H., AND YATES, D. J. C., *J. Catal.* **10**, 362 (1968).
4. CIMINO, A., BOUDART, M., AND TAYLOR, H. S., *J. Phys. Chem.* **58**, 796 (1954).
5. ANDERSON, J. R., AND BAKER, B. G., *Nature* (London) **187**, 937 (1960).

6. ANDERSON, J. R., AND BAKER, B. G., *Proc. Roy. Soc. Ser. A* **271**, 402 (1963).
7. ANDERSON, J. R., AND AVERY, N. R., *J. Catal.* **2**, 542 (1963).
8. ANDERSON, J. R., AND AVERY, N. R., *J. Catal.* **5**, 446 (1966).
9. ANDERSON, J. R., AND AVERY, N. R., *J. Catal.* **7**, 315 (1967).
10. KOCHLOEFL, K., AND BAZANT, V., *J. Catal.* **10**, 140 (1968).
11. KEMPLING, J. C., AND ANDERSON, R. B., *Ind. Eng. Chem., Process Des. Develop.* **9**, 116 (1970).
12. KIKUCHI, E., AND MORITA, Y., *J. Catal.* **15**, 127 (1969).
13. BARRON, Y., MAIRE, G., CORNET, D. M., AND GAULT, F. G., *J. Catal.* **2**, 152 (1963).
14. BARRON, Y., MAIRE, G., MULLER, J. M., AND GAULT, F. G., *J. Catal.* **5**, 428 (1966).
15. MULLER, J. M., AND GAULT, F. G., IV Int. Congr. Catal., IV Preprint No. 15, Moscow (1968).
16. BOUDART, M., AND PTAK, L. D., *J. Catal.* **16**, 90 (1970).
17. BOUDART, M., ALDAG, A. W., PTAK, L. D., AND BENSON, J. E., *J. Catal.* **11**, 35 (1968).